Probing the Microscopic Molecular Environment in Liquids: Intermolecular Dynamics of CS_2 in Alkane Solvents†

Dale McMorrow,* Napoleon Thantu,‡ Joseph S. Melinger, and Seong K. Kim‡,§

Naval Research Laboratory, Washington, D.C. 20375

William T. Lotshaw*

GE Research and Development, P.O. Box 8, RM. KWC-627, Schenectady, New York 12301

Received: February 23, 1996; In Final Form: April 16, 1996⊗

The femtosecond optical-heterodyne-detected optical Kerr effect/Raman-induced Kerr effect (OHD OKE/RIKE) dynamics of CS_2 dissolved in a series of alkane solvents are reported. The data reveal that the nondiffusive (subpicosecond) dynamics of simple molecular liquids are determined largely by the details of the local, microscopic environment, rather than by the bulk solution properties, with no correlation observed between the short-time, nondiffusive dynamics and the bulk solution viscosity. For each solvent investigated, the vibrational spectral density is observed to narrow and shift to lower frequency with increasing dilution. While the same general trend is observed for each solvent, deviations of magnitude are observed for the longer-chain *n*-alkanes. This, coupled with the markedly nonexponential decay of the orientational anisotropy observed for the higher-alkane dilutions, suggests the presence of two distinct environments in which isolated pockets of CS_2 exist. The observed spectral evolution is discussed in terms of a simple damped harmonic oscillator model in which the vibrational spectral densities are inhomogeneously broadened. This model allows for contributions from underdamped, critically damped, and overdamped oscillators that arise from a single vibrational degree of freedom. Analysis of the data in terms of this model reveals an exchange of spectral density from the higher-frequency underdamped oscillators to lower-frequency overdamped and critically damped oscillators, with the degree of inhomogeneity decreasing with increasing dilution.

I. Introduction

The role of intermolecular interactions in shaping the subpicosecond dynamics of molecular liquids is a topic of substantial importance to representations of the liquid state and remains a difficult question to assess from both experimental and theoretical perspectives. Femtosecond nonlinear optical (NLO) methods recently have developed into powerful tools fo the interrogation of molecular dynamics in optically transparent liquids. In particular, NLO methods involving optical heterodyne detection (OHD) techniques, such as the OHD optical Kerr effect (OKE) and Raman-induced Kerr effect (RIKE), can provide significant advantages over quadratic NLO methods and the more traditional frequency-domain techniques of spontaneous light scattering and far-infrared absorption.[1−10]

The role of the local environment in determining the intermolecular structure and dynamics of liquids can be revealed in a controlled fashion through dilution studies. In the case of ideal solutions, the molecules of a neat liquid are systematically replaced by solvent molecules, giving rise to an effectively continuous variation in the intermolecular potential seen by the original species. Previously, we reported on the OKE dynamics of CS_2 dissolved in effectively inert alkane solvents.[2] In this paper we extend that work to include new data and extend the analysis to include the Fourier-transform/deconvolution methods that separate the nuclear and electronic contributions to the measured transients.[3−5] When presented in the spectral density representation, these results provide a particularly clear picture of how the structure and dynamics of liquids are shaped by the microscopic molecular environment. Furthermore, the spectral density representation provides a natural interface to recent theoretical descriptions of liquid structure and dynamics, including instantaneous normal mode (INM) and Brownian oscillator descriptions.[11,12]

The results presented here largely corroborate the conclusions of our earlier report[2] and indicate that, even for the weakly interacting species of this study, on the femtosecond time scale, nondiffusive dynamics of liquids are determined largely by the details of the local, microscopic environment, rather than by the bulk solution properties. In particular, no correlation is observed between the short-time, nondiffusive dynamics and the bulk solution viscosity, whereas the picosecond time scale diffusive reorientational dynamics evolve in a manner that is consistent with changes in the bulk viscosity. The spectral density for the nondiffusive (vibrational) dynamics narrows and shifts to lower frequency upon dilution for each of the alkane solvents investigated, and the spectral shifts are consistent with those expected for intermolecular vibrational modes as the curvature of the effective intermolecular potential is reduced. The increased signal-to-noise (S/N) achieved with the newer Ti:sapphire laser technology reveals features that were not evident in the earlier data. In particular, when long-chain alkanes are used as solvents, we observe evidence for nonideality in the CS_2/alkane solutions that implies microscopic domains in which the CS_2 "probes" experience significantly distinct intermolecular potentials.

II. Experimental Section

The experimental apparatus and procedures have been discussed in detail;[1−5] only the essential features will be repeated

* To whom correspondence should be addressed.

† Presented at the Northeast Regional ACS Meeting in Rochester, NY (October 24 and 25, 1995), on the "Structure and Dynamics of Liquids".

‡ National Research Council Postdoctoral Fellow.

§ Permanent address: Department of Chemistry, Sung Kyun Kwan University Suwon, Republic of Korea.

⊗ Abstract published in *Advance ACS Abstracts,* May 15, 1996.

S0022-3654(96)00571-0 CCC: $12.00

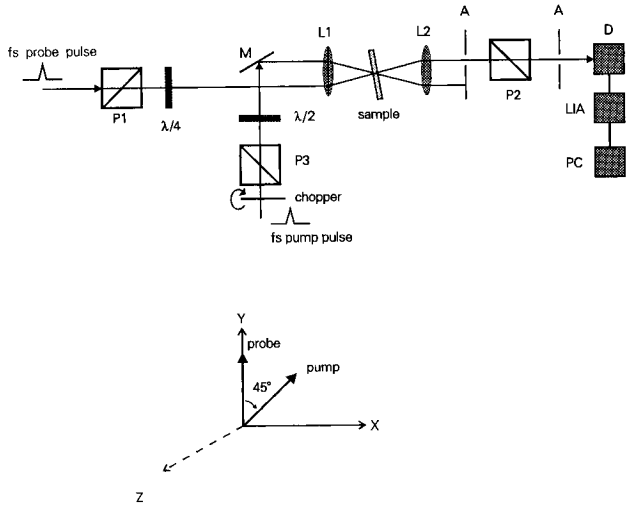

Figure 1. Experimental setup for performing the time-resolved OHD OKE/RIKES experiment: P, polarizer, L, lens; $\lambda/2$, half-wave plate; D, detector; LIA, lock-in amplifier; PC, personal computer.

here. Three different laser systems were used in this study. Early experiments utilized ~65 fs duration optical pulses centered at ~635 nm generated with a synchronously-pumped antiresonant-ring dye laser (~15 mW average power at an 82 MHz repetition rate[13]). More recent experiments have used the output of two different Ti:sapphire lasers: one that is synchronously pumped[10] and the second self-mode-locked, both of which generate 20−40 fs nearly transform-limited optical pulses centered around 800 nm. Within the S/N constraints and temporal resolution differences of the different systems, the agreement between different results is excellent.

The OHD OKE/RIKE experimental setup is shown schematically in Figure 1. The implementation of optical heterodyne detection is straightforward in an OKE/RIKE experiment. With the $\lambda/4$ wave plate positioned between the crossed polarizers oriented with its "fast" axis parallel to the polarization plane of the probe beam, a slight rotation ($<1°$) of the input polarizer will introduce a small orthogonal polarization component (the local oscillator) that is 90° out-of-phase with the probe field.[1−5] The transmission of the Kerr cell is detected with a photodiode (or photomultiplier tube)/lock-in-amplifier combination and recorded as a function of the delay between the pump and probe pulses. The pure heterodyne responses are constructed from data scans collected with positively and negatively sensed local oscillators, which eliminates the homodyne contamination of the heterodyne signal.[5,14] The sense of the local oscillator is determined by the sign of the input polarizer rotation. This method is in contrast to that described by Scherer and coworkers,[9,15] who rotate the $\lambda/4$ wave plate and thereby introduce a mixed-phase local oscillator. Using Jones matrices, it is easy to show that the mixed-phase local oscillator cannot distinguish between birefringent and dichroic contributions to the heterodyne signal.[5]

III. Fourier-Transform Relationships

The theoretical developments associated with the optical heterodyne-detected optical Kerr effect experiment and the relevant Fourier-transform relationships have been described in detail elsewhere,[3−5] and only the essential expressions will be repeated here. The transmission function for the Kerr cell for Fourier-transform-limited optical pulses and out-of-phase optical heterodyne detection is described by the relation

$$T(\tau) = \int_{-\infty}^{\infty} G_0^{(2)}(\tau - t)\ \mathrm{Re}\ \chi_{\mathrm{eff}}^{(3)}(t)\ \mathrm{d}t = G_0^{(2)}(\tau) * R_{\mathrm{eff}}(\tau) \quad (1)$$

where $G_0^{(2)}(\tau)$ is the background-free laser pulse intensity autocorrelation function, $R_{\mathrm{eff}}(t) \propto \mathrm{Re}\ \chi_{\mathrm{eff}}^{(3)}(t)$ is the time-domain impulse response function of the medium, and the asterisk (*) indicates a convolution operation. Fourier transformation of (1) gives rise to the frequency-domain product

$$F\{T(\tau)\} = T(\Delta\omega) = F\{G_0^{(2)}(\tau)\}\ F\{R_{\mathrm{eff}}(\tau)\} \quad (2)$$

where the $F\{\ \}$ indicate Fourier-transform operations. Equation 2 describes the spectral filter effects of finite-bandwidth optical pulses on the intrinsic frequency response of a material. The effects of spectral filtering on the OKE of CS_2 liquid are illustrated in Figure 3 (vide infra). The NLO frequency response spectrum of the material, $\chi_{\mathrm{eff}}^{(3)}(\Delta\omega)$, is generated by deconvolution of the spectral-filter effects of the finite-bandwidth laser pulse by evaluation of the complex quotient

$$\chi_{\mathrm{eff}}^{(3)}(\Delta\omega) = \xi F\{R_{\mathrm{eff}}(t)\} = \xi \frac{F\{T(\tau)\}}{F\{G_0^{(2)}(\tau)\}} \quad (3)$$

where $\Delta\omega = \omega_m \pm \omega_n$, the $\omega_{m,n}$ are Fourier components of the pump pulse, and ξ is a constant. The two functions on the right-hand side (rhs) of (3) are experimentally measured quantities. The frequency range over which eq 3 has sufficient S/N to render meaningful results is determined by the coherence bandwidth of the laser pulses and the quality of the data. Typically, this range is 2−3 times the fwhm laser bandwidth for transform-limed pulses. For the 30 fs Ti:sapphire pulses used in these studies the range is ~800 cm^{-1}, and for the 65 fs dye laser pulses, ~325 cm^{-1}. In either case, the usable bandwidth is significantly greater than that of the CS_2 NLO response.

In this study our primary interest is in the nuclear part of the NLO response. The nuclear and electronic contributions can be separated on the basis of symmetry by recognizing that[3]

$$R_{\mathrm{nuc}}(t) = 2F^{-1}\{\mathrm{Im}\ \chi_{\mathrm{eff}}^{(3)}(\Delta\omega)\} H(t - t_0) \quad (4)$$

where $H(t)$ is the Heaviside step function and $R_{\mathrm{nuc}}(t)$ is the nuclear part of the impulse response function. All of the information on the nuclear response of the material to the optical pulses is contained in the spectral density function, $\mathrm{Im}\ \chi_{\mathrm{eff}}^{(3)}(\Delta\omega)$.[3] The nuclear contribution to the measured transient, $T_{\mathrm{nuc}}(\tau)$, can then be generated with the relation[3]

$$T_{\mathrm{nuc}}(\tau) = G_0^{(2)}(\tau) * R_{\mathrm{nuc}}(\tau) \quad (5)$$

IV. Historical Background: Spectral Filter Effects in Neat CS_2

The spectral-filter effects of finite-duration, finite-bandwidth optical pulses have had a significant impact on the shape and interpretation of measured NLO transient wave forms.[3,16−20] As pulse durations evolved from the picosecond to the femtosecond regime over the past three decades, the NLO dynamics of CS_2 liquid often were used as a benchmark to evaluate the new technology. The historical evolution of the time-resolved OKE of CS_2, therefore, provides an interesting study of the impact of spectral-filter effects on the understanding of molecular dynamics in liquids. In this section we discuss the historical

evolution of the time-resolved optical Kerr effect in CS_2 in the context of our present understanding of molecular dynamics in liquids.

Early work on the time-resolved optical Kerr effect utilized picosecond optical pulses and was carried out in the quadratic (or homodyne) configuration.[22−24] With picosecond duration pulses, only the diffusive reorientational contributions to the OKE signal are accessible, and much early work focused on the utility of the OKE for use in optical shutters.[22] Two useful articles addressing this early work are presented in refs 23 and 24.

The first measurement to successfully resolve the picosecond time scale relaxation of CS_2 was the study of Ippen and Shank at Bell Laboratories in 1975.[16] Using ∼1 ps duration pulses in the quadratic OKE configuration, an asymmetric waveform was observed. To verify that the asymmetry was associated with the response of the liquid, and not with an asymmetry of the laser pulses, an optical heterodyne experiment in which the Kerr cell was "biased half open" with a quarter-wave plate was performed. This linearized the OKE signal in the NLO response of the liquid and confirmed that the 2.1 ± 0.3 ps decay was associated with the reorientational relaxation of CS_2. To our knowledge, this represents the first implementation of optical heterodyne detection techniques (although the terminology was not introduced until a later date[25,26]).

The presence of a subpicosecond decay component in the NLO response of CS_2 liquid was first evident in data published in 1980.[17] Those authors, however, incorrectly identified the fast relaxation with the instantaneous electronic response, with the observed asymmetry identified as arising from an asymmetry in their laser pulses.[17,18] It was later recognized that pulse durations of <100 fs are required to resolve the electronic contribution to the OKE in CS_2.[21] In 1982 the subpicosecond relaxation of CS_2 was clearly resolved and identified as arising from nuclear degrees of freedom.[19,20] Using different, but closely related, techniques, groups from Cornell and Bell Labs measured time constants of 330 and 240 fs, respectively. In 1987, using 65 fs duration optical pulses, we reported a time constant of 160 fs for the same relaxation.[21] The lack of agreement between the different measurements of the same liquid could not be accounted for in terms of the quoted ±20 fs experimental errors and was not immediately resolved.

Independent of the work by the Bell Labs group noted above,[16] the theoretical background associated with optical heterodyne detection techniques was worked out and demonstrated experimentally for the CW case by Levenson and coworkers in the late 1970s.[25,26] That formalism was utilized and applied to the time-resolved OKE experiment in 1987.[21] The advantages of OHD over the quadratic OKE configuration include the following: an increased signal amplitude and improved signal-to-noise ratio over quadratic NLO methods;[25,26] the signal amplitude is linear, rather than quadratic, in $\chi^{(3)}$, resulting in the elimination of troublesome cross-terms, making data analysis more straightforward;[1−5,21,25,26] the detected signal is linear in both the pump and probe pulse intensities;[1−5,25,26] and for Fourier-transform limited optical pulses the effective instrument function is the experimentally measured laser pulse intensity autocorrelation function. This latter attribute makes deconvolution procedures possible without any detailed pulse shape information and permits the separation of nuclear and electronic contributions to the measured waveform.[1−5] A comparison of the OHD and quadratic OKE response for CS_2 measured under otherwise identical conditions is presented in ref 5. The distinction between the experimental setup used by the Bell Labs groups[16,19] and that used by us[1−5] lies in the implementation of the local oscillator. In the former case, a circularly polarized probe beam is used to bias the Kerr cell "half open" through a rotation of the $\lambda/4$ waveplate (*cf. Figure* 1), while in the latter the probe is made only slightly elliptically polarized through a small rotation of the input polarizer. Questions of S/N aside, the significant difference between the two configurations is associated with the nature of the detected signal. The circularly polarized probe results in a complex (mixed-phase) local oscillator, with the detected signal containing both birefringent and dichroic contributions. The local oscillator introduced by tipping off the input polarizer is 90° out-of-phase with the probe field, resulting in a purely birefringent signal ($Re\ \chi^{(3)}$). For transparent liquids such as CS_2, the dichroic contributions are typically small, and the distortion of the waveform associated with the mixed-phase configuration is not severe. These considerations have been discussed in detail recently.[5]

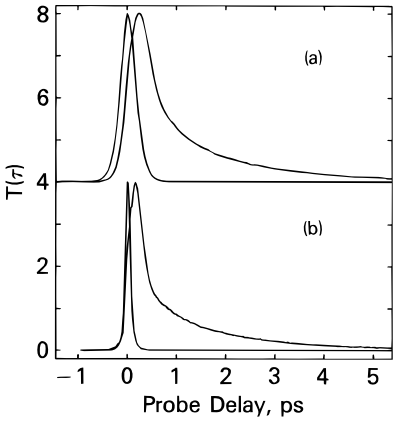

Figure 2. OHD OKE/RIKES signal measured for CS_2 liquid at 295 K for fwhm pulse durations of (a) 225 and (b) 65 fs. Also included are the intensity autocorrelation functions for each pulse width measured at the sample position. The curves are offset vertically for clarity. Dye laser data.

The discrepancies in the measured time constants for the fast relaxation of CS_2 can be addressed naturally in terms of spectral-filter effects. Figure 2 illustrates the pulse width dependence of the OHD OKE of CS_2. Also shown for each curve is the laser pulse intensity autocorrelation function measured at the sample position, which defines the experimental bandwidth and the experimental time origin. The upper curve of Figure 2 gives the CS_2 OHD OKE transient for ∼225 fs excitation and probing pulses (∼350 fs autocorrelation width) and is similar to the data presented in earlier work.[19,20] The lower curve was obtained with 65 fs laser pulses (100 fs autocorrelation width) and is analogous to more recent data.[2,5,6,21] At long times both transients decay exponentially with a time constant of 1.6−1.7 ps that is characteristic of reorientational diffusion in CS_2.

In Figure 3 we show the experimental spectral density functions for three different excitation conditions (solid curves), together with the relevant filter functions, which are given by the Fourier transform of the autocorrelation function, $F\{G_0^{(2)}(\tau)\}$ (dashed curves). These data illustrate graphically the spectral-filter effects of the finite-duration pump and probe laser pulses on the intrinsic frequency response of CS_2. The upper curve in Figure 3 illustrates the nuclear response of CS_2 to a δ-function optical pulse. For δ-function excitation $F\{G_0^{(2)}(\tau)\}$ is a constant function of $\Delta\omega$. This spectrum was obtained by direct application of eq 3 to the 65 fs pulse width data of Figure 2. Evident is a narrow, low-frequency feature that is associated with the decay of the orientational anisotropy and a broad, higher-frequency band extending to ∼120 cm^{-1}. This latter feature is associated with the subpicosecond, intermo-

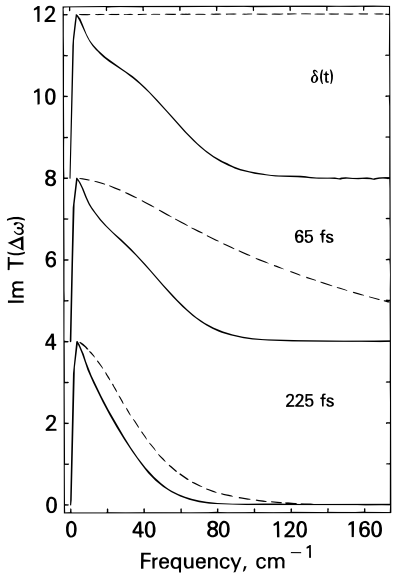

Figure 3. Imaginary part of the OHD OKE/RIKES spectral density functions for three different pulse width conditions. The upper curve is the intrinsic spectral density generated from the 65 fs experimental data of Figure 2. The two lower curves correspond to the experimental data of Figure 2. The dashed curves are the filter functions relevant to each pulse width and represent the experimental bandwidth for each case. The curves are offset vertically for clarity.

lecular dynamics of the liquid and constitutes the spectral density of the coherently excited, intermolecular oscillators.[3−5]

The spectral-filter effects of finite-duration, finite-bandwidth laser pulses on the intrinsic dynamics of CS_2 are illustrated by the two lower sets of curves. The spectra Im $T(\Delta\omega)$ (where $T(\Delta\omega) = F\{T(t)\}$) can be generated by either of two procedures: (i) by application of eq 2 to the intrinsic spectral density (upper curve, Figure 3) using the functions $F\{G_0^{(2)}(\tau)\}$ (dashed curves in Figure 3) generated from the experimentally measured pump/probe correlation functions that are shown in Figure 2, or (ii) more directly, by taking the imaginary part of the Fourier transform of the experimental data, Im $F\{T(\tau)\}$. The spectra of Figure 3 were produced with the latter method, although both yield the same result. The Im $T(\Delta\omega)$ curves of Figure 3 are the frequency-domain representation of the nuclear part of the CS_2 transient OKE experiment, with the lower two spectra illustrating grahically the spectral filtering of the intrinsic frequency response by the finite duration optical pulses. For 65 fs excitation and probing pulses the effective experimental bandwidth (dashed curve) is sufficiently greater than that of the intrinsic material response, and the spectral-filter effect is only moderate. With 225 fs laser pulses, however, a gross distortion of the intrinsic response is evident; only a lower-frequency subensemble of oscillators contributes to the detected signal. The higher-frequency oscillators are *not excited* by the narrower-bandwidth, longer-duration pulses.

The large variation in the published time constants for the NLO response of CS_2 noted above is described naturally in the frequency-domain picture in terms of pulse-width-dependent spectral-filter effects: as the pulse width is increased, a progressively narrower ensemble of oscillators is excited, giving rise to less destructive interference and a slower inhomogeneous dephasing time. Thus, with 65 fs laser pulses a relaxation of ∼160 fs that is characteristic of the inhomogeneous width of the CS_2 librational response is observed. For longer duration pulses the higher-frequency oscillators are filtered out, resulting in the slower apparent decay times reported in ref 19 and 20. It is necessary to discuss briefly the results of ref 20 in more detail. That work quoted a pulse duration of 70 fs, in apparent

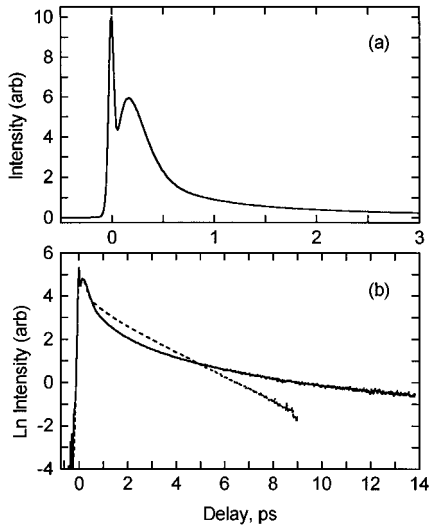

Figure 4. OHD OKE/RIKES measured for a 10% solution of CS_2 in *n*-hexadecane solvent plotted in linear and semilogarithmic format. A normalized OHD OKE/RIKES transient measured for neat CS_2 is included for reference (dashed curve). Ti:sapphire data.

disagreement with the conclusions of the previous paragraphs. Because those experiments were performed with the two different outputs of the CPM laser, however, the relevant parameter is the cross-correlation function, which exhibits a fwhm duration of 190−200 fs.[20]

The time constants measured in ref 19−21 are related to the distribution of oscillators that is excited and probed with the optical pulses used in the respective experiments (*cf.* eq 2). Each of the results, however, is distorted by the pulse-width-dependent spectral-filter effects, and none are representative of the intrinsic spectral density. The results obtained with the shortest optical pulses, however, possess sufficient bandwidth that deconvolution procedures can be utilized successfully to generate the intrinsic frequency response of CS_2 liquid, as is shown in Figure 3, and had been verified recently using 30 fs optical pulses generated with a Ti:sapphire laser.[5] Attempts to deconvolute the 225 fs data of Figure 2 to extract the intrinsic spectral density were unsuccessful.

V. Femtosecond OKE Dynamics of CS_2/Alkane Solutions

An extensive series of experiments have been performed for dilutions of CS_2 in a series of alkane solvents, including *n*-pentane, isopentane (2-methylbutane), isoheptane (2-methylhexane), *n*-tetradecane, and *n*-hexadecane. A preliminary report on some of these results has been presented previously.[27] The general features of the dilutions data are similar to those reported previously for neat CS_2.[1,2,5,6,21] Figure 4 shows an OHD OKE transient measured for a 10% solution of CS_2 in *n*-hexadecane solvent presented in linear and logarithmic format. Evident are the pulse-width-limited contribution of the electronic hyperpolarizability, the temporally delayed and rapidly relaxing contribution that has been identified with the nondiffusive intermolecular dynamics, followed by the slower, picosecond time scale diffusive relaxation of the laser-induced orientational anisotropy. For the *n*-hexadecane data of Figure 4, the diffusive reorientational contribution is notably nonexponential for delays greater than *ca.* 3 ps. This is in contrast to the OKE dynamics of neat CS_2 and solutions of CS_2 in the shorter-chain alkanes such as *n*-pentane, which exhibit single-exponential decays on the picosecond time scale.[2,5,28] The data of Figure 4 can be fitted for delays greater than 3 ps to a biexponential decay law with time constants of ∼4 and ∼25 ps (longer scans were used

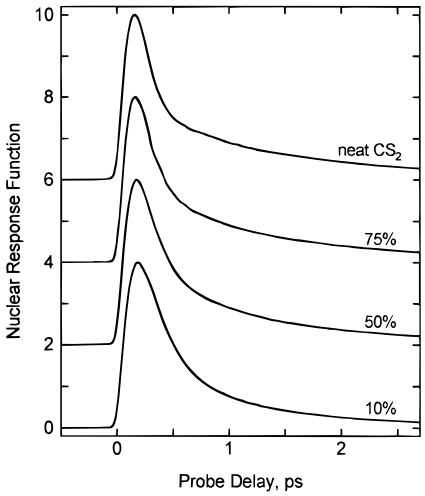

Figure 5. Nuclear part of the OHD OKE/RIKES transient (normalized) for solutions of CS_2 in *n*-pentane solvent measured at 24 °C. The electronic contribution was removed using the Fourier-transform relationships described in section III. The curves are offset vertically for clarity. Ti:sapphire data.

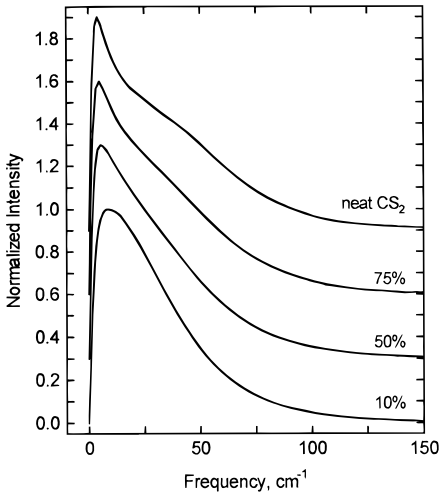

Figure 6. Intrinsic (deconvoluted) OKE/RIKES spectral density functions, Im $\chi^{(3)}(\Delta\omega)$, for the CS_2/*n*-pentane solutions of Figure 5 illustrating significant spectral evolution on dilution. The curves are offset vertically for clarity.

for this determination). A similar biexponential decay is observed for dilutions of CS_2 in *n*-tetradecane solvent. The nonexponential character of the relaxation that is evident in Figure 4 was not detectable in the data of our earlier report due to the S/N limitations of those data at the higher dilutions.[2] This observation is important for interpretation of the subpicosecond dynamics and is discussed in greater detail below.

Figure 5 shows the nuclear part of the OHD OKE transients for the CS_2/*n*-pentane dilution series. These transients were generated from the raw OHD OKE data using the Fourier-transform methods noted above.[3−5] The changes in the time-domain transients on dilution are quite subtle, with some broadening and redistribution of intensity evident with increasing dilution. Similar trends are observed for the other alkane solvents investigated.

The frequency-domain representation reveals more clearly the spectral evolution that occurs when CS_2 is diluted in an alkane solvent. Figure 6 shows the frequency-domain representation of the *n*-pentane data shown in Figure 5. The spectra of Figure 6 contain all of the information on the nuclear response of the liquid to a δ-function optical pulse (for the frequency region shown). For *neat* CS_2, two distinct contributions are evident:

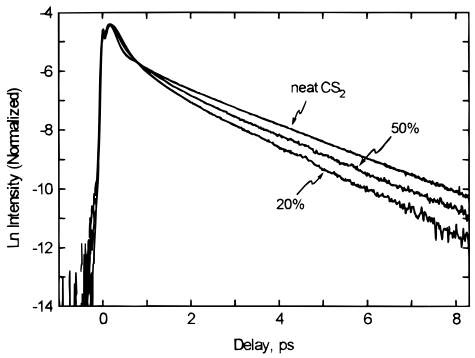

Figure 7. Femtosecond OHD OKE/RIKES transients for the *n*-pentane dilution series plotted in a semilogarithmic format. Ti:sapphire data.

a sharp, low-frequency feature associated with the 1.7 ps diffusive relaxation of the orientational anisotropy and a broad, diffuse band that can be identified with the nondiffusive intermolecular dynamics.[5] On dilution in the weakly interacting *n*-pentane solvent, the diffusive peak broadens, while the spectral distribution of the nondiffusive band shifts to lower frequency. At the lowest dilution investigated (10%), these two bands overlap significantly, and only a single, structureless band is discernible in the spectral density distribution. The broadening of the diffusive peak is consistent with the shorter relaxation time observed for reorientation in the lower-viscosity *n*-pentane solution.[2]

The dependence of the picosecond dynamics on dilution is illustrated Figure 7, which shows data for the *n*-pentane dilution series plotted in a semilogarithmic format. For solutions of *n*-pentane, isopentane, and isoheptane, at delays greater than 3 ps, the OHD OKE/RIKES response relaxes by a single-exponential decay law. The deviations from exponentiality for the longer chain alkanes are noted above. The data of Figure 7 reveal a decrease in the exponential time constant with decreasing CS_2 concentration, consistent with the expectations for reorientational diffusion as the solution viscosity is decreased on dilution. The results for isopentane dilution are qualitatively similar. For dilutions with the higher-viscosity solvents the opposite trend is observed (*cf.* Figure 4). The diffusive reorientational time constant is effectively unchanged throughout the isoheptane dilution series, for which the viscosity remains unchanged on dilution.[2]

One concern regarding experiments of this type is the possible distortion of the measured transient by contributions from the solvent. In a recent study, the intramolecular vibrational modes of CCl_4 were used as an internal reference, permitting the solvent contribution to be removed from the solution response.[29b] In the current experiments, however, because of the large nonlinearity of CS_2, the solvent contribution remains largely insignificant for CS_2 concentrations down to 10%. This is illustrated in the data of Figure 8, which shows the OKE dynamics measured for a 20% solution of CS_2 in *n*-pentane compared to that of neat *n*-pentane measured under identical experimental conditions. Near $\tau = 0$ the electronic contribution originating from the *n*-pentane solvent is significant, but that contribution is rigorously removed from the data with the Fourier-transform analysis and does not affect the interpretation of the data. At a delay of 200 fs the nuclear part of the *n*-pentane OKE intensity is approximately 0.05 that of the CS_2/*n*-pentane solution. Also, the nondiffusive contribution to the *n*-pentane OKE decays more rapidly than that of the CS_2 solutions, and by 500 fs the *n*-pentane OKE is approximately 2 orders of magnitude weaker than that of the 20% CS_2/*n*-pentane solution. However, the data of Figure 8b reveal that the solvent OKE decays more slowly than that of the solution on the picosecond time scale. This

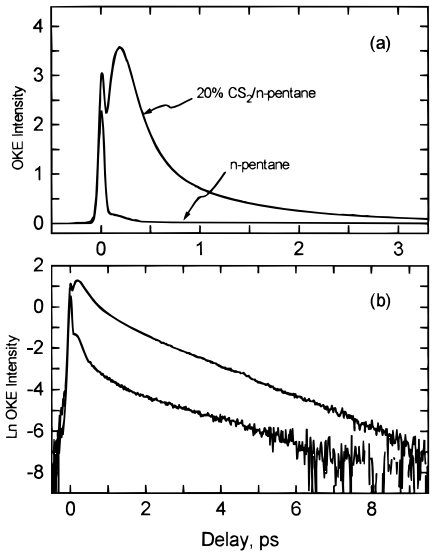

Figure 8. Femtosecond OHD OKE/RIKES transients for 20% CS_2 in *n*-pentane and for neat *n*-pentane solvent plotted in linear and semilogarithmic formats. Ti:sapphire data.

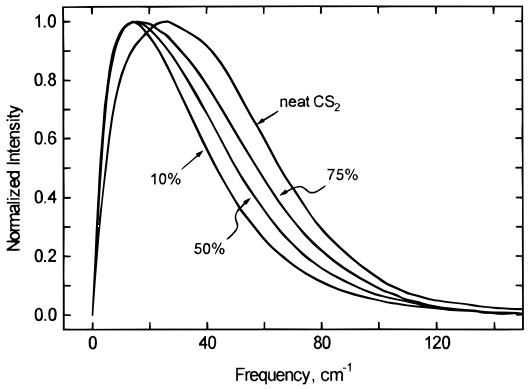

Figure 9. Vibrational OHD OKE/RIKES spectral density functions for the *n*-pentane dilution series of Figure 5. The diffusive reorientational contribution was removed from the time-domain data prior to the Fourier-transform procedure.

gives rise to distortions of the OKE at large delays. For the 20% CS_2/*n*-pentane solution, for example, deviations from nonlinearity originating from the solvent background become evident for delays greater than ~9 ps and are evident in the 10% CS_2/*n*-pentane OKE for delays of ~8 ps. This signal distortion is of very low amplitude and has a negligible effect on the spectral density functions.

The nondiffusive contributions are of particular interest since they reflect the local intermolecular potential, and hence the local structure, probed by individual CS_2 molecules. Assuming that the reorientational relaxation can be described by a diffusion equation, that contribution can be removed from the data in a straightforward fashion, as has been described elsewhere.[1−5] The resulting spectra for the CS_2/*n*-alkane dilution series, which contain only the nondiffusive contributions to the dynamics, are shown in Figure 9. Plotted in this fashion, the changes in the vibrational spectral density are particularly clear: *the intermolecular vibrational distribution narrows and shifts to lower frequency with increasing alkane concentration*. The changes are quite significant: the band maximum shifts from 26.5 cm^{-1} in neat CS_2 to 15 cm^{-1} in the 10% solution, while the bandwidth decreases from 60 to 40 cm^{-1}. The observed shifts of the spectral distribution with increasing dilution are consistent with those expected for an intermolecular vibrational mode as the effective intermolecular potential changes when

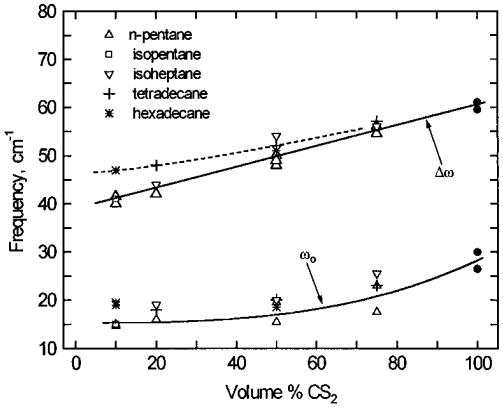

Figure 10. The fwhm bandwidth, $\Delta\omega$, and peak frequency, ω_0, plotted against the solution concentration for each of the solutions investigated. The lines are included to guide the eye. This figure contains both dye laser and Ti:sapphire laser data for temperatures ranging from 20 to 24 °C.

CS_2 molecules are replaced by the weakly interacting pentane molecules. Recall that CS_2-CS_2 interactions are largely due to induced dipole and large permanent quadrupole moments of the CS_2 molecule, whereas the multipole moments of the alkanes are vanishingly small in comparison.[30]

Each of the solvents investigated exhibits the general trends evident in the data of Figure 9: the nondiffusive spectral density narrows and shifts to lower frequency on dilution, irrespective of the bulk solution viscosity. Peak position and bandwidth data for each of the solutions investigated are plotted in Figure 10. To generate the data of Figure 10, the full width at half-maximum bandwidths, $\Delta\omega$, and the peak frequencies, ω_0, were determined directly from nondiffusive spectral density functions such as those of Figure 9. The lines are included to guide the eye. These data reveal that while the diffusive reorientation times reflect the bulk viscosity of the solutions in accordance with the qualitative expectations of the Debeye−Stokes−Einstein theory, there is no correlation between the nondiffusive intermolecular dynamics and the bulk solution viscosity. As CS_2 molecules are replaced by more weakly interacting alkane molecules on dilution, the net effect for all solvents investigated is a flattening of the intermolecular potential, giving rise to the observed shift of the spectral density to lower frequencies. Since the interactions induced by the different alkane molecules are similar, the observed agreement between the different liquids is reasonable. The scatter in the data of Figure 10 arises from several sources. Data were collected on three different laser systems with sample temperatures ranging from 20 to 24 °C. Consistent with recent temperature-dependent measurements on neat CS_2,[5] the higher temperature (24 °C) data exhibit systematically lower bandwidths and band maxima than data collected at 21 °C.[2] Also, earlier data collected with the dye laser system[2] exhibit inferior S/N characteristics to the more recent Ti:sapphire data, giving rise to greater uncertainty.

The conclusions of the previous paragraph are based on the assumption that the nondiffusive spectral density is associated with intermolecular vibrational degrees of freedom. Such low-frequency spectral density is often discussed in terms of free rotational (or inertial) motion. We note that in the free rotation limit the intermolecular potential is flat in the angular coordinate of interest, and therefore, the molecular spectra are dependent only on temperature. No spectral changes are expected on dilution at constant temperature in the free rotation limit. The spectral evolution evident in the data of Figures 9 and 10 is consistent with that expected for intermolecular vibrational degrees of freedom as the intermolecular potential is modified

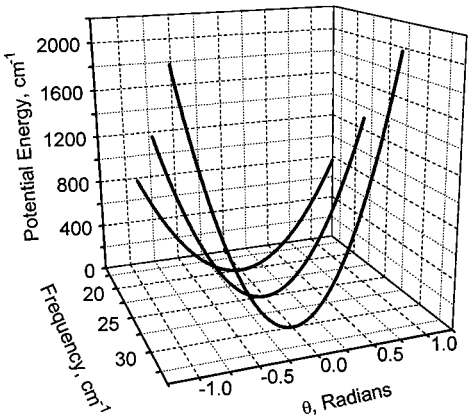

Figure 11. Schematic harmonic oscillator potential energy diagrams illustrating the change curvature of the intermolecular potential function for oscillators of frequencies 30, 25, and 20 cm^{-1}.

and is inconsistent with the presence of free rotational motion in liquid CS_2. Similar conclusions recently have been drawn for benzene based on a comparison of the measured OHD OKE spectrum with that calculated for free rotational motion.[5] The vibrational degrees of freedom most likely to contribute to the intermolecular OKE intensity are due to molecular libration and the interaction-induced intensity that is associated with translational degrees of freedom.

The effect of dilution on the average intermolecular potential experienced by CS_2 molecules in solution is illustrated schematically in Figure 11. To generate this figure, the average peak positions for three different solute concentrations were taken from the data of Figure 10, and the potential functions in units of wavenumber were calculated in the harmonic approximation using the expressions

$$V(\theta) = {}^1/_2 k\theta^2 \tag{6a}$$

where

$$k = 4\pi^2 cI\omega_0{}^2/h \tag{6b}$$

and ω_0 is the peak frequency in wavenumbers, c is the speed of light, h is Planck's constant, and I is the molecular moment of inertia of CS_2, which is taken to be 256.4×10^{-40} g cm^2.[31]

While the data of Figure 10 illustrate that the spectral shifts are similar for each of the alkane solvents used, inspection reveals a systematic deviation from this trend for the longer-chain *n*-alkane solvents at the higher dilutions (*cf.* dashed line in Figure 10). This observation is made explicit in the data of Figure 12, which compares the nondiffusive spectral density functions for 10% and 50% solutions of CS_2 in *n*-pentane and *n*-hexadecane. As is evident, for a given solution composition, the spectral density functions for the *n*-hexadecane solutions are broader and shifted to higher frequencies than those of the *n*-pentane solutions. This effect is evident for the 50% solutions and becomes quite pronounced for the 10% solutions. The nonexponential decay of the orientational anisotropy that is observed for solutions involving the longer-chain alkanes (*cf.* Figure 4) provides some insight into this apparent discrepancy. A nonexponential decay of the orientational anisotropy cannot be explained in terms of the single-molecule degrees of freedom associated with the high-symmetry CS_2 molecule. However, a nonexponential decay can be accounted for if the solution is nonideal in that the local concentrations of solvent and solute vary within a macroscopic volume. The biexponential character of the picosecond relaxations of the higher dilutions of CS_2 in *n*-tetradecane and *n*-hexadecane suggests the presence of at least

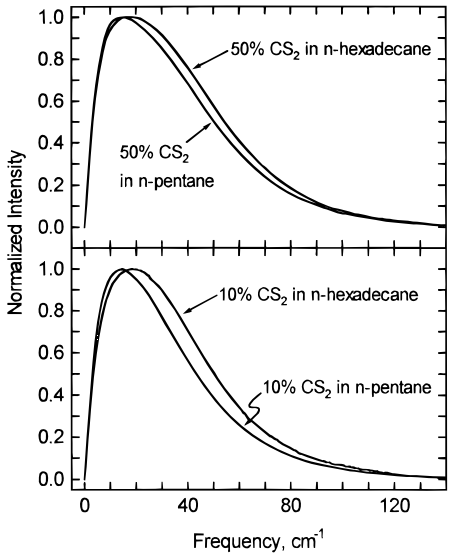

Figure 12. Nondiffusive 24 °C OHD OKE/RIKES spectral density functions for 50% (upper) and 10% (lower) solutions of CS_2 in isopentane and *n*-hexadecane. Ti:sapphire data.

two distinct environments in these solutions. The slower time constant is in agreement with that expected diffusive reorientation at the viscosities in question. However, the ~4 ps time constant of the faster component is similar to that of neat CS_2 liquid at 298 K, suggesting that isolated pockets of CS_2 are present in the solution. The presence of CS_2 pockets also will affect the subpicosecond contributions to the measured waveforms. In particular, the measured dynamics will reflect a superposition of higher-frequency contributions from those molecules in a predominantly CS_2 environment and lower-frequency contributions that arise from CS_2 molecules in predominantly alkane environments. The net effect would be a nondiffusive spectral density that is intermediate between the two extremes. Since the spectral densities measured for the shorter-chain alkane solvents *n*-pentane, isopentane, and isoheptane are nearly identical for a given CS_2 concentration, the deviation from this trend in the longer-chain alkane solutions suggests inhomogeneity in those solutions.

The explication of this effect may lie in the internal degrees of freedom of the alkane solvents, coupled with the differences in the electronic interactions associated with CS_2-CS_2, CS_2-alkane, and alkane−alkane interactions. The longer *n*-alkanes possess a higher number of internal degrees of freedom which result in complex and diverse globular configurations of individual molecules. Unless the interaction between CS_2 and the alkane is specific, the CS_2 will likely populate the interstices of single long-chain alkane molecules, as well as those of the tangled intermolecular structures arising from alkane−alkane interactions. In these environments, configurations of CS_2 molecules will be determined (in part) by steric constraints: where multiple CS_2 molecules can be accommodated in the local structure, CS_2-CS_2 interactions will predominate, and the corresponding spectral density will exhibit characteritics of the spectrum of neat CS_2. Those sites in which CS_2 is isolated will exhibit the spectral density due to the weaker interactions with the alkane solvent and reflect the local elastic properties as well.

The present results provide evidence for the existence of microscopic domains in the CS_2/alkane solutions. A more detailed understanding of the precise nature of the different types of solvent/solute configurations within the liquid will benefit from a detailed investigation into the picosecond time scale relaxations of the longer-chain alkane solutions, together with computer modeling efforts. In particular, on the basis of the

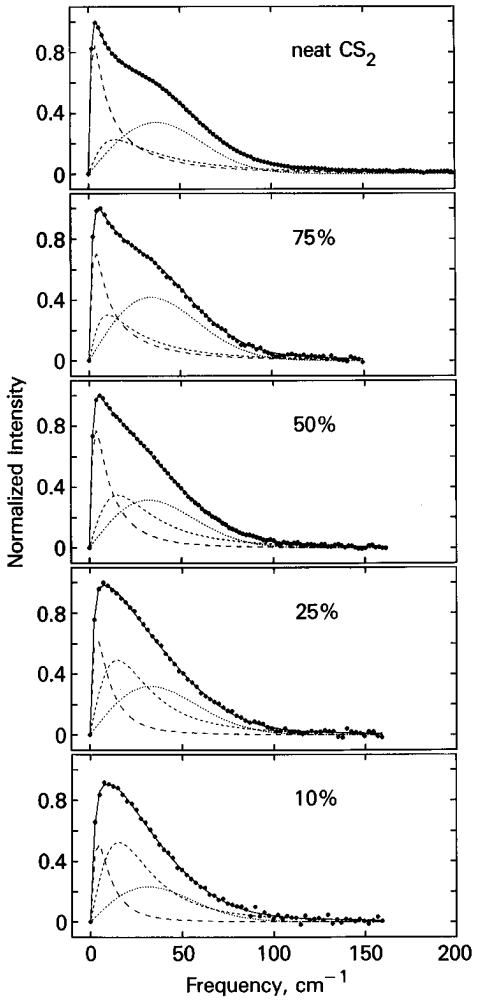

Figure 13. OHD OKE/RIKES spectral density functions for the *n*-pentane dilution series fitted to a sum of two Lorentzians and a Gaussian. The Gaussian is the higher-frequency curve in each case. Dye laser data.

present results, it is not clear whether the picosecond dynamics of the longer-chain alkane solutions are best described as biexponential or stretched exponential. Whereas a biexponential decay law would be consistent with two distinct CS_2 environments, a stretched exponential decay would be indicative of a continuous distribution of microscopic structures in the liquid. These issues will be addressed in future work.

To this point we have focused on the qualitative and quantitative trends reflected in the intermolecular spectral density of CS_2 on dilution with effectively inert alkane solvents. It is also useful to perform a curve-fitting analysis to generate a modal decomposition of the spectral density and to further investigate the effects of dilution on the dynamics of CS_2. Figure 13 shows the spectral density functions for the CS_2/*n*-pentane dilution series (*cf.* Figure 6) fitted to a sum of two Lorentzians and a Gaussian. The current frequency-domain curve-fitting analysis is similar, but not identical to our earlier time-domain analysis,[2] with the primary difference being that the two Lorentzian functions utilized to generate the data of Figure 13 do not contain inertial effects. This shortcoming is insignificant to any of the conclusions drawn from this analysis.

Each spectrum of Figure 13 is decomposed into three contributions: a narrow Lorentzian that together accounts for the picosecond time-scale relaxation of the orientational anisotropy and a broader Lorentzian and a Gaussian that account for the subpicosecond contributions to the spectral density. The diffusive reorientation time constant was determined from the

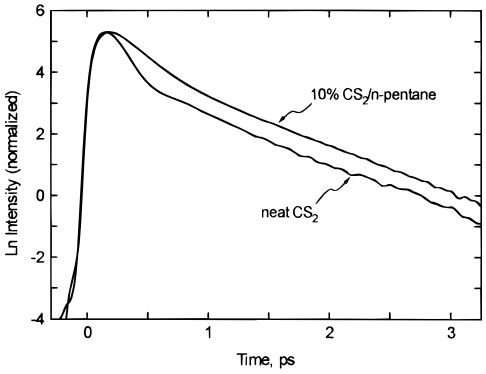

Figure 14. Normalized nondiffusive part of OHD OKE/RIKES transients for neat CS_2 and a 10% solution of CS_2 in *n*-pentane illustrating the exchange of intensity between the faster and slower contributions on dilution. Ti:sapphire data.

time-domain data and is held fixed in the curve-fitting analysis. The presence of two distinct time-scale subpicosecond relaxation components in the OKE of CS_2 is well established.[1,5,32] The time constant of the ~500 fs quasi-exponential relaxation was determined from the time-domain analysis and held fixed in the curve-fitting procedure as well. Figure 14 shows the subpicosecond nuclear dynamics of a 10% solution of CS_2 in *n*-pentane compared to that of neat CS_2, illustrating that the bimodal character remains intact even at the higher dilutions. To obtain the data of Figure 14, the nuclear and electronic contributions were separated using the Fourier-transform methods described above, and the orientational anisotropy was tail matched and subtracted off using the procedure described previously.[1−5]

The physical origin of the two subpicosecond relaxations evident in the data of Figure 14 (and the curve-fitting analysis of Figure 13) can be addressed in terms of a simple harmonic oscillator model in which the intermolecular vibrational spectral densities are inhomogeneously broadened and can exhibit underdamped, critically damped, and overdamped contributions.[13] The vibrational excitation, $Q(t)$, may be represented as linear superposition of the Fourier components of the vibrational ensemble that are coherently excited by the optical pulse(s)

$$Q(t) = \sum_i \langle q_i^a(t)\rangle + \sum_i \langle q_i^b(t)\rangle + \sum_i \langle q_i^c(t)\rangle \qquad (7)$$

where $\langle q_i(t)\rangle$ is the ensemble-averaged vibrational coherence for the *i*th homogeneously broadened vibrational coordinate, and the labels *a*, *b*, and *c* indicate the different damping conditions in eq 7. If we consider a system of driven, damped harmonic oscillators, then the $\langle q_i(t)\rangle$ take on the form

$$\langle q_i^a(t)\rangle = Ae^{-\gamma t}\sin(\omega_i t) \qquad \omega_{0i} > \gamma \qquad (8a)$$

$$\langle q_i^b(t)\rangle = Bte^{-\gamma t} \qquad \omega_{0i} = \gamma \qquad (8b)$$

$$\langle q_i^c(t)\rangle = Ce^{-\gamma_i t}[1 - e^{-2\omega_i t}] \qquad \omega_{0i} < \gamma \qquad (8c)$$

where $\omega_{0i}/2\pi$ is the characteristic (undamped) frequency of the *i*th oscillator, γ is a phenomenological damping/dephasing rate, $\omega_i = |\omega_{0i}^2 - \gamma^2|^{1/2}$, $\gamma_i = \gamma - \omega_i$, the three cases labeled *a*, *b*, and *c* correspond to underdamped, critically damped, and overdamped motion, respectively, and any frequency dependence of γ is neglected.

Much of the physical intuition regarding vibrational dynamics derives from the higher-frequency, underdamped, isolated

resonances of intramolecular vibrational modes. Such resonances are described by the first term on the right-hand side (rhs) of eq 7. For a homogeneously broadened transition only a single term in the sum over *i* will contribute, typically resulting in the widely recognized Lorentzian line shape.

Much of this intuition may not be applicable to intermolecular resonances. For intermolecular vibrational coordinates the intermolecular motions that are responsible for dephasing are of the same physical origin and exhibit a similar frequency dependence to that of the coordinates themselves.[32] Further, the same motions can give rise to inhomogeneities in the local environments such that

$$\omega_0 \approx \Delta\omega \approx \gamma \tag{9}$$

where $\Delta\omega$ is the width of the inhomogeneous distribution. When ω_0, γ, and $\Delta\omega$ are all of the same magnitude, all three terms of eq 7 can contribute to the observed dynamics (and line shape) for a single, inhomogeneously broadened vibrational degree of freedom, giving rise to a dynamical profile consisting of both oscillatory and dissipative contributions. The dissipative contributions, represented by the second and third terms on the rhs of eq 7, *add constructively at all times*, resulting in a quasi-exponential relaxation with the time constant determined by γ and the ω_{0i}. The oscillatory contributions, described by the first term on the rhs of eq 7, experience destructive interference, giving rise to a rapid relaxation that is dependent on the inhomogeneous width, $\Delta\omega$. The degree of oscillatory character evident in the measured waveform, therefore, is dependent on the spectral density of the underdamped motions represented by term *a* of eq 7.

Referring again to Figure 13, the Gaussian function can be identified as arising from the underdamped contributions to the dynamics (term *a* of (7)). The high-frequency Lorentzian can be identified with contributions from terms *b* and *c* of eq 7. This analysis suggests that for neat CS_2 the nondiffusive dynamics are predominantly underdamped, with a small contribution arising from overdamped and critically damped oscillators. In contrast, for the 10% solution the dominant contribution is from overdamped and critically damped oscillators, with a relatively small contribution arising from underdamped oscillators. A similar trend is evident in the time-domain curve-fitting analysis presented previously for isoheptane solvent.[2] The significance of this observation is discussed further below.

VI. Discussion

The interpretation of the subpicosecond contributions to the CS_2 dilution data is as follows. As the nearest neighbors surrounding a "probe" CS_2 molecule are replaced by weaker-interacting alkane molecules, the curvature of the average intermolecular potential seen by the "probe" is decreased, as illustrated schematically in Figure 11. This results in a shift of the nondiffusive spectral density to lower frequencies, as is evident in the data of Figure 9. Analysis of the experimental data suggests that the dephasing rate, γ_i, is effectively unchanged throughout the dilution series,[2] and it reasonably may be assumed that γ is constant as well. With γ constant the spectral density shifts to lower frequency on dilution, and an exchange of intensity is observed from the higher-frequency underdamped contributions to the lower-frequency overdamped and critically damped contributions. Such an exchange of intensity is evident in the curve-fitting results of Figure 13, with the intermediate-frequency Lorentzian gaining intensity at the expense of the higher-frequency Gaussian function. This exchange of intensity is also evident in the reduced time domain data of Figure 14, in which the amplitude and time constant of the fast relaxation are reduced significantly in the 10% data when compared to those of neat CS_2.

Earlier work on the subpicosecond dynamics of CS_2 has suggested that the dynamics are inhomogeneously broadened.[1,2,5,6,32−34] The evolution in the CS_2 OKE line shape as a function of alkane concentration supports that assertion. Equation 7 does not assume that the line shape is inhomogeneously broadened, but is consistent with that possibility. The need to consider more than a single term on the rhs of (7) in the analysis of the dilution data is consistent with some degree of inhomogeneous broadening. In this regard, within the framework of the model described here, the temporal signature of the reduced data of Figure 14 can be considered characteristic of low-frequency inhomogeneously broadened transitions. In particular, the two-component character of the subpicosecond dynamics, with a faster, Gaussian-like relaxation followed by a slower quasi-exponential decay, is indicative of an inhomogeneously broadened transition in the mixed-damping regime. The ratio of the two time constants can be used to give an indication of the degree of imhomogeneity. In this regard, the data of Figure 14 indicate clearly that the 10% CS_2/*n*-pentane vibrational spectral density is distinctly less inhomogeneous than that of the neat CS_2 solution. This interpretation is particularly straightforward for high-symmetry species such as CS_2, in which only a single librational mode is Raman-active.

A recent series of experiments by Tominaga and co-workers probed the fifth-order contributions to the nonlinear optical susceptibility and also addressed the inhomogeneity of the CS_2 spectral density.[35−37] In their initial report[35] it was concluded that the transitions contributing to the OKE in CS_2 are purely homogeneously broadened. More recent experiments,[36,37] which produced higher-quality data, indicate that some degree of inhomogeneity exists in the spectral density of neat CS_2. Those authors also have performed a series of dilutions of CS_2 in alkane solvents which suggest that the degree of inhomogeneity decreases with increasing dilution, in agreement with the conclusions noted above and our earlier report.[2] Very recently, fifth-order experiments on CS_2 and benzene also have been presented by Steffen and Duppen.[38]

Several factors must be considered for a detailed interpretation of either the $\chi^{(3)}$ OKE data or the $\chi^{(5)}$ Raman echo data. First is the nature of the orientational anisotropy. Because this contribution is not vibrational in origin, it should not be considered as part of the vibrational line shape. If considered, however, it must be treated as homogeneously broadened. Similarly, any overdamped and critically damped contributions to the line shape must be viewed as homogeneously broadened as well. The underdamped contributions, which are represented by the Gaussian function in Figure 13, can contain both homogeneous and inhomogeneous broadening contributions. The recent analysis of Tominaga *et al.*,[35−37] for example, does not distinguish between overdamped and underdamped vibrational contributions and therefore might overestimate the degree of homogeneous broadening of the vibrational spectral density.

In our earlier analyses[2,32] it was assumed that the homogeneous dephasing rate was independent of frequency across the band and that the homogeneous dephasing rate of the underdamped oscillators could be approximated by the measured decay time of the overdamped contributions. These assumptions lead to[31] an upper limit of 3 for the ratio $\Delta\omega_I/\Delta\omega_H$ of the inhomogeneous to homogeneous contributions to the line width for neat CS_2. Since this ratio is determined from the ratio of the fast and slow decay times of the vibrational dynamics (*cf.* Figure 14), the ratio of 3 applies only to the inhomogeneity of

the *underdamped* contributions to the line shape. This value, therefore, cannot be compared directly to the conclusions of ref 36 regarding the degree of inhomogeneity for CS_2.

To compare the results of this analysis to the conclusions of Tominaga *et al*., it is necessary to include line-broadening contributions from overdamped and critically damped oscillators. When these contributions are considered for neat CS_2 the degree of inhomogeneity is reduced somewhat, in better agreement with the conclusions of ref 36. Applying a similar analysis to the dilution data reveals that, when the line shape is taken as a whole, the degree of inhomogeneity decreases significantly on dilution, with the ratio $\Delta\omega_I/\Delta\omega_H$ approaching 0.2 for the 10% CS_2/*n*-pentane solution. Thus, analysis of the dilution data in terms of eq 7 and the concepts discussed here suggests that while the intermolecular vibrational spectral density for neat CS_2 exhibits a significant degree of inhomogeneous broadening, the line shape for the 10% CS_2/*n*-pentane solution is predominantly homogeneously broadened, in agreement with the trend reported in ref 37. It is interesting to note that, when only the underdamped contributions are considered, the degree of inhomogeneity changes only moderately on dilution, with the ratio $\Delta\omega_I/\Delta\omega_H = 1.3$ for the 10% CS_2/*n*-pentane solution, as determined from the time-domain data of Figure 14. This is also evident in the data of Figure 13, in which the width of the Guassian function changes only moderately on dilution. The data of Figure 13 suggest that the significant decrease in the degree of inhomogeneity that is deduced from the line shape as a whole is a consequence of the exchange of intensity between the underdamped and overdamped contributions on dilution, with the overdamped/critically damped contributions playing the dominant role in determining the line shape at the higher dilutions.

One significant conclusion can be made from this analysis: while it is evident the degree of inhomogeneity of the CS_2 spectral density decreases on dilution in alkane solvents, it is not unequivocal that the decrease is a consequence of a reduction in the distribution of molecular environments in the solution, as it is tempting to assume. In particular, an analysis of the vibrational spectral density (*e.g*., Figures 9, 10, and 12) suggests that the apparent decrease in inhomogeneity is a consequence of a redistribution of spectral density from the inhomogeneously broadened underdamped oscillators, into lower-frequency overdamped and critically damped oscillators, for which there is no apparent method for determining the degree of inhomogeneity. This redistribution of spectral density is a consequence of the shifting of the intermolecular potential on dilution, as is discussed above (*cf*. Figure 11).

The modal decomposition described above and shown in Figure 13 can be extended by the use of line shape functions appropriate to Brownian oscillators.[12] With a multimode Brownian oscillator model for the intermolecular spectral density distribution, the analyses presented above and in our previous reports[1,2,5,32] on intermolecular interactions in CS_2 can be related to the recently developed theoretical representation for mode-coupling effects in nonlinear optical spectroscopies like OHD OKE/RIKE.[12] In this representation Tanimura, Mukamel, and co-workers[12] have constructed the nonlinear optical response functions for $\chi^{(3)}$, $\chi^{(5)}$, and $\chi^{(7)}$ under conditions of varying mode coupling, and these constitute the theoretical basis for the fifth-order Raman echo experiments recently conducted by Tominaga et al.[35−37] Such experiments propose to directly distinguish the homogeneous and inhomogeneous line shape contributions to the vibrational spectral density and were applied to the librational coordinate of CS_2. One significant aspect of the Tanimura and Mukamel theory is the explicit appearance of a term in the nonlinear response functions for $\chi^{(3)}$, $\chi^{(5)}$, and $\chi^{(7)}$ processes which arises from collective mode dynamics. For $\chi^{(3)}$, the forms of the nonlinear response function with and without mode coupling (to the quadratic limit) are

$$R^{(3)}(\tau) = \frac{2i\alpha_1^{\,2}}{\hbar}\int d\Gamma\, S(\Gamma)\, C''(\tau,\Gamma) \tag{10}$$

and

$$R^{(3)}(\tau) = \frac{2i\alpha_1^{\,2}}{\hbar}\int d\Gamma\, S(\Gamma)\, C''(\tau,\Gamma) + \frac{2i\alpha_2^{\,2}}{\hbar}\int d\Gamma\, S(\Gamma)\, C''(\tau,\Gamma)\, C'(\tau,\Gamma) \tag{11}$$

where α_1^2 and α_2^2 represent the magnitude of the polarizability correlation function in the absence and presence of mode coupling (in the quadratic coupling limit here), respectively. The *C* terms in the integrands are the correlation functions of the nuclear coordinates:

$$C''(\tau,\Gamma) = \int d\omega\, J(\omega,\Gamma)\sin(\omega\tau) \tag{12a}$$

and

$$C'(\tau,\Gamma) = \int d\omega'\, J(\omega',\Gamma)\cos(\omega'\tau)\coth(\beta\hbar\omega'/2) \tag{12b}$$

where $C''(\tau,\Gamma)$ and $C'(\tau,\Gamma)$ are the imaginary and real parts of the correlation function for the nuclear degrees of freedom; $S(\Gamma)$ and $J(\omega,\Gamma)$ are the multimode inhomogeneous and homogeneous distribution functions; Γ is the set of inhomogeneous parameters describing the oscillator frequency, coupling strength, and damping; $\beta = 1/kT$; and ω is the frequency of the homogeneous oscillators. Equation 10 gives the response function $R^{(3)}(\tau)$ in the limit where the polarizability is a linear function of the nuclear coordinates of the medium and shows that the vibrational spectral density of the response is given by a simple convolution of the homogeneous and inhomogeneous line shape contributions:

$$I(\omega) = \int d\Gamma\, S(\Gamma)\, J(\omega,\Gamma) \tag{13}$$

When the polarizability is nonlinear in the nuclear coordinates due to intermode coupling, the $R^{(3)}(\tau)$ acquires additional contributions such as the second term of eq 11, which scale differently with respect to the order of the homogeneous distributions:

$$I(\omega) = \int d\Gamma\, S(\Gamma)\, J(\omega,\Gamma) + \int d\Gamma\, S(\Gamma)\, J(\omega,\Gamma)\int d\omega'\, J(\omega',\Gamma)\coth(\beta\hbar\omega'/2) \tag{14}$$

The second integral term in (11) exhibits many of the dynamic and spectral characteristics of the "reorientational" mode commonly described by the Debye−Stokes−Einstein representation: the spectral density of the second term is biased to the lower-frequency modes in $S(\Gamma)$ by the hyperbolic cotangent thermal weighting factor, thereby reflecting the line shape of the lowest-frequency mode(s) near the peak and the higher-frequency coupled modes in the wings. This term can explicitly account for collective contributions to the reorientational coordinate(s) and the transition between inertial and collisionally averaged temporal regimes. In comparing the multimode Brownian oscillator representation to the spectral decomposition presented above and in our previous reports, it is important to recognize that (i) the second integral term of eq 14 is not due

to a single (orientational) nuclear coordinate, but includes contributions from several (or all) modes of the medium, and (ii) the reorientational coordinate still contributes to the response function through the first integral (linear) term of $R^{(3)}(\tau)$ with a relative amplitude determined by the ratio of α_1^2 and α_2^2. Despite the fact that the $R^{(3)}(\tau)$ in the presence of mode coupling does not rigorously allow elimination of the contribution from a single nuclear coordinate by subtraction of a single response function (as in our tail matching procedure), from a practical perspective such an approach is a good first-order approximation. The rigorously correct procedure involves a substantial numerical analysis of the measured $R^{(3)}(\tau)$ at a series of values of a state variable, such as temperature, where the scaling of the $S(\Gamma)$ and $J(\omega,\Gamma)$ are understood.[39] In a forthcoming report we will examine the quality of the "tail-matching" approximation, mode couplings, the effects of qualitative mode damping, and the predictions for the $\chi^{(5)}$ Raman echo response[12] for neat CS_2 and the CS_2/alkane solutions within the multimode Brownian oscillator analysis.[40]

VII. Conclusions

The optical heterodyne-detected OKE/RIKES dynamics of CS_2 dissolved in a series of alkane solvents is reported. These data reveal that the nondiffusive (subpicosecond) dynamics of simple molecular liquids are determined largely by the details of the local, microscopic environment, rather than by the bulk solution properties. No correlation is observed between the short-time, nondiffusive dynamics and the bulk solution viscosity, whereas the picosecond time scale diffusive reorientational dynamics evolve in a manner that is consistent with changes in the bulk viscosity. Presentation of the data in the spectral density representation provides a clear picture of the spectral evolution on dilution in the various solvents investigated. For each solvent investigated, the spectral density is observed to narrow and shift to lower frequency with increasing dilution. While the same general trend is observed for each solvent, deviations of magnitude are observed for the longer-chain *n*-alkanes. This, coupled with the markedly nonexponential decay of the orientational anisotropy observed for the higher-alkane dilutions, suggests the presence of two distinct environments in which isolated pockets of CS_2 exist.

The spectral shifts observed on dilution are discussed in terms of a simple damped harmonic oscillator model in which the vibrational spectral densities are inhomogeneously broadened. This model permits contributions from underdamped, critically damped, and overdamped oscillators associated with a single vibrational degree of freedom. Analysis of the data in terms of this model reveals an exchange of spectral density from the higher-frequency underdamped oscillators into lower-frequency overdamped and critically damped oscillators, with the degree of inhomogeneity decreasing with increasing dilution.

Acknowledgment. The authors acknowledge the useful comments by the referees and thank Kei Tominaga for making his manuscripts available to us prior to publication.

References and Notes

(1) McMorrow, D.; Lotshaw, W. T.; Kenney-Wallace, G. A. *IEEE J. Quantum Electron.* **1988**, *QE-24*, 443.

(2) Kalpouzos, C.; McMorrow, D.; Lotshaw, W. T.; Kenney-Wallace, G. A. *Chem. Phys. Lett.* **1988**, *150*, 138; **1989**, *155*, 240.

(3) McMorrow, D.; Lotshaw, W. T. *Chem. Phys. Lett.* **1990**, *174*, 85. McMorrow, D. *Opt. Commun.* **1990**, *86*, 236.

(4) McMorrow, D.; Lotshaw, W. T. *J. Phys. Chem.* **1991**, *95*, 10395.

(5) Lotshaw, W. T.; McMorrow, D.; Thantu, N.; Melinger, J. S.; Kitchenham, R. *J. Raman. Spectrosc.* **1995**, *26*, 571.

(6) Hattori, T.; Kobayashi, T. *J. Chem. Phys.* **1991**, *24*, 3332.

(7) Chang, Y. J.; Castner, E. W., Jr. *J. Chem. Phys.* **1993**, *99*, 113.

(8) Chang, Y. J.; Castner, E. W., Jr. *J. Chem. Phys.* **1993**, *99*, 7289.

(9) Cho, M.; Du, M.; Scherer, N. F.; Fleming, G. R.; Mukamel, S. *J. Chem. Phys.* **1993**, *99*, 2410.

(10) Palese, S.; Schilling, L.; Miller, R. J. D.; Staver, P. R.; Lotshaw, W. T. *J. Phys. Chem.* **1994**, *98*, 308.

(11) Buchner, M.; Ladanyi, B. M.; Stratt, R. M. *J. Chem. Phys.* **1992**, *97*, 8522.

(12) Tanimura, Y.; Mukamel, S. *J. Chem. Phys.* **1993**, *99*, 9496.

(13) Lotshaw, W. T.; McMorrow, D.; Dickson, T.; Kenney-Wallace, G. A. *Opt. Lett.* **1989**, *14*, 309.

(14) Dickson, T. R. PhD Thesis, University of Toronto, 1991.

(15) Vohringer, P.; Scherer, N. F. *J. Phys. Chem.* **1995**, *99*, 2684.

(16) Ippen, E. P.; Shank, C. V. *Appl. Phys. Lett.* **1975**, *26*, 92.

(17) Etchpare, J.; Grillon, G.; Antonetti, A.; Orzag, A. Inn *Picosecond Phenomena II*; Springer: New York, 1980; pp 123−127.

(18) Etchpare, J.; Grillon, G.; Martin, J. L.; Bruneau, C.; Antonetti, A. In *Picosecond Phenomena III*; Springer: New York, 1982; pp 217−220.

(19) Green, B. I.; Farrow, R. C. *J. Chem. Phys.* **1982**, *77*, 4779; *Chem. Phys. Lett.* **1983**, *98*, 273.

(20) (a) Halbout, J. M.; Tang, C. L. *Appl. Phys. Lett.* **1982**, *40*, 765. (b) In *Time Resolved Vibrational Spectroscopy*; Atkinson, G., Ed.; Academic: New York, 1983; pp 73−82.

(21) Kalpouzos, C.; McMorrow, D.; Lotshaw, W. T.; Kenney-Wallace, G. A. *J. Phys. Chem.* **1987**, *91*, 2028. Lotshaw, W. T.; McMorrow, D.; Kalpouzos, C.; Kenney-Wallace, G. A. *Chem. Phys. Lett.* **1987**, *136*, 323.

(22) Dunguay, M. A.; Hansen, J. W. *Appl. Phys. Lett.* **1969**, *15*, 92.

(23) Sala, K.; Richardson, M. C. *Phys. Rev. A* **1972**, *12*, 1036.

(24) Ho, P. P.; Alfano, R. R. *Phys. Rev. A* **1979**, *20*, 2170.

(25) Eesley, G. L.; Levenson, M. D.; Tolles, W. M. *IEEE J. Quantum Electron* **1978**, *QE-14*, 45. Levenson, M. D.; Eesley, G. L. *Appl. Phys.* **1979**, *19*, 1.

(26) Levenson, M. D. *Introduction to Nonlinear Laser Spectroscopy*; Academic: New York, 1982.

(27) McMorrow, D.; Kim, S. K.; Melinger, J. S.; Lotshaw, W. T. In *Ultrafast Phenomena VIII*; Springer: Berlin, 1992; pp 656−657.

(28) Lotshaw, W. T.; McMorrow, D.; Kenney-Wallace, G. A. *Proc. SPIE* **1988**, *981*, 20.

(29) (a) McMorrow, D.; Lotshaw, W. T. *Chem. Phys. Lett.* **1993**, *201*, 369. (b) Lotshaw, W. T.; Staver, R.; McMorrow, D.; Thantu, N.; Melinger, J. S. In *Ultrafast Phenomena IX*; Springer: Berlin, 1994; pp 91−92.

(30) Madden, P. A. In *Ultrafast Phenomena*, Vol. 4; Auston, D. H., Eisenthal, K. B., Eds.; Springer: Berlin, 1985; pp 244−251. Geiger, L. C.; Ladanyi, B. M. *Chem. Phys. Lett.* **1989**, *159*, 413. Reynolds, L.; Gardecki, J. A.; Frankland, S. J. V.; Maroncelli, M. *J. Phys. Chem.* **1996**, *100*, 10337.

(31) Herzberg, G. *Infrared and Raman Spectra of Polyatomic Molecules*; D. Van Nostrand: New York, 1945; p 369.

(32) McMorrow, D.; Lotshaw, W. T. *Chem. Phys. Lett.* **1991**, *178*, 69.

(33) Ruhman, S.; Williams, L. T.; Joly, A. G.; Kohler, B.; Nelson, K. A. *J. Phys. Chem.* **1987**, *91*, 2237.

(34) Ruhman, S.; Joly, A. G.; Nelson, K. A. *IEEE J. Quantum Electron* **1988**, *QE-24*, 460.

(35) Tominaga, K.; Naitoh, Y.; Kang, T. J.; Yoshihara, K. In *Ultrafast Phenomena IX*; Springer: Berlin, 1994; pp 143−144. Tominaga, K.; Yoshihara, K. *Phys. Rev. Lett.* **1995**, *74*, 3061.

(36) Tominaga, K.; Keogh, G. P.; Naitoh, Y.; Yoshihara, K. *J. Raman. Spectrosc.* **1995**, *26*, 495. Tominaga, J. K.; Yoshihara, K. *J. Chem. Phys.* **1996**, *104*, 4419.

(37) Tominaga, K.; Yoshihara, K. *J. Chem. Phys.* **1996**, *104*, 1159.

(38) Steffen, T.; Duppen, K. *Phys. Rev. Lett.* **1996**, *76*, 1224.

(39) Palese, S.; Buontempo, J.; Schilling, L.; Miller, R. J. D.; Tanimura, Y.; Mukamel, S.; Lotshaw, W. T. *J. Phys. Chem.* **1994**, *98*, 12466.

(40) Lotshaw, W. T.; McMorrow, D.; Melinger, J. S.; Thantu, N. To be published.

JP9605717